

PAPER

Development of interatomic potentials appropriate for simulation of devitrification of $\text{Al}_{90}\text{Sm}_{10}$ alloy

To cite this article: M I Mendelev *et al* 2015 *Modelling Simul. Mater. Sci. Eng.* **23** 045013

View the [article online](#) for updates and enhancements.

Related content

- [Molecular dynamics simulation of solidification and devitrification in a one-component system](#)
M I Mendelev
- [Solute–solute correlations responsible for the prepeak in structure factors of undercooled Al-rich liquids: a molecular dynamics study](#)
Feng Zhang, Yang Sun, Zhuo Ye *et al.*
- [An angular embedded atom method interatomic potential for the aluminum–silicon system](#)
P Saidi, T Frolov, J J Hoyt *et al.*

Recent citations

- [Nucleation kinetics in Al-Sm metallic glasses](#)
L. Zhao *et al*
- [Structural hierarchy as a key to complex phase selection in Al-Sm](#)
Z. Ye *et al*
- [Nanoglasses: A New Kind of Noncrystalline Material and the Way to an Age of New Technologies?](#)
Herbert Gleiter

Development of interatomic potentials appropriate for simulation of devitrification of $\text{Al}_{90}\text{Sm}_{10}$ alloy

M I Mendelev¹, F Zhang¹, Z Ye¹, Y Sun^{1,3}, M C Nguyen¹,
S R Wilson¹, C Z Wang¹ and K M Ho^{1,2}

¹ Division of Materials Sciences and Engineering, Ames Laboratory, Ames, IA, 50011, USA

² Department of Physics, Iowa State University, Ames, Iowa 50011, USA

³ Hefei National Laboratory for Physical Sciences at the Microscale and Department of Physics, University of Science and Technology of China, Hefei, Anhui 230026, People's Republic of China

E-mail: mendelev@ameslab.gov

Received 7 October 2014, revised 30 March 2015

Accepted for publication 6 April 2015

Published 23 April 2015




CrossMark

Abstract

A semi-empirical potential for the $\text{Al}_{90}\text{Sm}_{10}$ alloy is presented. The potential provides satisfactory reproduction of pure Al properties, the formation energies of a set of Al–Sm crystal phases with Sm content about 10%, and the structure of the liquid $\text{Al}_{90}\text{Sm}_{10}$ alloy. During molecular dynamics simulation in which the liquid alloy is cooled at a rate of 10^{10} K s^{-1} , the developed potential produces a glass structure with lower *ab initio* energy than that produced by *ab initio* molecular dynamics (AIMD) itself using a typical AIMD cooling rate of $8 \cdot 10^{13} \text{ K s}^{-1}$. Based on these facts the developed potential should be suitable for simulations of phase transformations in the $\text{Al}_{90}\text{Sm}_{10}$ alloy.

Keywords: semi-empirical potentials, molecular dynamics simulation, liquid/glass structure

 Online supplementary data available from stacks.iop.org/MSMSE/23/045013/mmedia

(Some figures may appear in colour only in the online journal)

1. Introduction

The Al–Sm alloy is an interesting example of a system in which the width of the glass-forming region, centered at about 10% Sm, is limited to just a few atomic percent [1]. Since

the process competing with vitrification is solidification, this means that for some reason the nucleation/growth of crystal phases is difficult in this concentration region. According to the phase diagram [2], the stable crystal phases are fcc Al and Al₃Sm, but different metastable crystal phases can appear during solidification/devitrification [3, 4]. To analytically describe possible phase transformation pathways in Al₉₀Sm₁₀, knowledge of the driving forces for all possible phase transformations, atomic diffusivities in all phases and all relevant interface properties are needed. While the driving forces and atomic diffusivities can be obtained from *ab initio* calculations, determination of the properties of interfaces between different phases requires using classical molecular dynamics (MD) simulation [5] and therefore, employing semi-empirical potentials. Moreover, even the determination of the unit cell of a crystal phase may require a semi-empirical potential if the unit cell is sufficiently large, in which case *ab initio* calculations that test all possible candidates can become too expensive (e.g. see [6]). To our best knowledge, there are currently no semi-empirical potentials suitable for simulation of the structure and interface properties in Al–Sm alloys. In the present paper, we present a semi-empirical potential suitable for simulations of solidification/devitrification in the Al₉₀Sm₁₀ alloy.

Any potential appropriate for simulating phase transformations should be very computationally efficient, yet at the same time reproduce the main material properties. The most popular types of potentials employed to simulate phase transformations in metallic systems are embedded atom method (EAM) [7] and Finnis–Sinclair (FS) potentials [8]. EAM and FS potentials are comparable to pair potentials with respect to computational efficiency, but can properly reproduce important properties that pair potentials cannot (e.g. non-zero difference between the cohesive and unrelaxed vacancy formation energies and non-zero Cauchy pressure). In the present study we choose the FS type. The total potential energy in this formalism takes the following form:

$$U = \sum_{i=1}^{N-1} \sum_{j=i+1}^N \varphi_{t_i t_j}(r_{ij}) + \sum_{i=1}^N \Phi_{t_i}(\rho_i), \quad (1)$$

where t_i is the elemental type of atom i , N is the number of atoms in the system, $r_{i,j}$ is the separation between atoms i and j , $\varphi_{t_i t_j}(r)$ is the pairwise potential, $\Phi_{t_i}(\rho)$ is the embedding energy function and

$$\rho_i = \sum_j \psi_{t_i t_j}(r_{ij}), \quad (2)$$

where $\psi_{t_i t_j}(r)$ are density functions.

The rest of this paper is organized as follows. First, we describe *ab initio* calculations of the formation energy of Al–Sm crystal phases at $T = 0$ and *ab initio* molecular dynamics (AIMD) simulation used to obtain the density and partial pair correlation functions (PPCF) of liquid Al₉₀Sm₁₀ alloy at $T = 1273$ K. Next we present the potential development procedure. Finally, we test the reliability of the developed potential by creating an Al₉₀Sm₁₀ glass model and comparing its energy with AIMD data and the liquid-glass transition temperature with the experimental data.

2. *Ab initio* molecular dynamics simulation of the structure of liquid Al₉₀Sm₁₀ alloy

A series of Al-rich crystalline compounds with Sm composition close to 10% were included in the potential development procedure. In addition to the known stable or metastable phases

Table 1. Lattice parameters and formation energies of crystal phases included in the development of the FS potential. Pure Al and Sm were taken as the reference states in calculation of the formation energy. The top value is from the *ab initio* calculations and the bottom one is the value reproduced by the FS potential.

Phase	x_{Sm}	Structure type	a (Å)	b (Å)	c (Å)	$\alpha(^{\circ})$	$\beta(^{\circ})$	$\gamma(^{\circ})$	$\Delta(\text{eV/atom})$
Al	0	Fm $\bar{3}$ m	4.041	4.041	4.041	90.0	90.0	90.0	0
		(No.225)	4.041	4.041	4.041	90.0	90.0	90.0	0
Al ₄₅ Sm ₅	0.100	P1	9.749	9.866	9.782	88.8	89.7	93.4	−0.089
			9.713	9.965	9.657	88.2	88.4	92.5	−0.075
Al ₄₄ Sm ₅	0.100	P1	9.949	9.711	9.435	90.1	89.6	91.4	−0.098
			9.917	9.697	9.430	90.0	90.0	91.0	−0.100
α -Al ₄₂ Sm ₅	0.106	P1	9.791	9.612	9.326	90.0	90.0	90.1	−0.104
			9.818	9.463	9.414	90.0	90.0	90.1	−0.121
β -Al ₄₂ Sm ₅	0.106	P1	9.619	9.624	9.467	90.0	90.0	92.8	−0.098
			9.818	9.463	9.414	90.0	90.0	90.1	−0.121
γ -Al ₄₂ Sm ₅	0.106	P1	9.836	9.542	9.360	90.8	91.1	89.9	−0.104
			9.818	9.464	9.464	90.0	90.0	89.9	−0.121
Al ₄₀ Sm ₆	0.130	P1	9.814	9.263	9.537	90.0	90.0	90.0	−0.160
			9.895	9.289	9.464	90.0	90.0	90.0	−0.169
α -Al ₃₈ Sm ₇	0.156	P1	9.653	9.498	9.415	90.0	90.1	90.0	−0.198
			9.691	9.443	9.401	90.0	90.1	90.0	−0.185
β -Al ₃₈ Sm ₇	0.156	P1	9.499	9.653	9.415	89.9	90.4	89.9	−0.198
			9.443	9.691	9.401	89.9	90.0	90.0	−0.185
α -Al ₄₀ Sm ₈	0.167	P1	9.780	9.801	9.801	90.3	91.3	88.7	−0.228
			9.801	9.823	9.823	90.8	90.9	89.1	−0.182
β -Al ₄₀ Sm ₈	0.167	P1	9.328	10.780	9.358	90.0	90.0	90.0	−0.190
			9.366	10.340	9.560	90.0	90.0	90.0	−0.193
Al ₅ Sm	0.167	P6/mmm	4.598	4.597	6.356	90.0	90.0	120.0	−0.276
		(No.191)	4.569	4.569	6.430	90.0	90.0	120.0	−0.200
α -Al ₄ Sm	0.200	I4/mmm	4.242	4.242	11.349	90.0	90.0	90.0	−0.277
		(No.139)	4.238	4.238	11.292	90.0	90.0	90.0	−0.212
β -Al ₄ Sm	0.200	Imma	6.401	4.468	13.789	90.0	90.0	90.0	−0.338
		(No.74)	6.429	4.4584	13.891	90.0	90.0	90.0	−0.258
Al ₁₁ Sm ₃	0.214	Immm	4.364	9.929	12.946	90.0	90.0	90.0	−0.362
		(No.71)	4.352	10.080	12.941	90.0	90.0	90.0	−0.279
Al ₃ Sm	0.250	P6 ₃ /mmc	6.455	6.455	4.572	90.0	90.0	120.0	−0.447
		(No.194)	6.385	6.385	4.640	90.0	90.0	120.0	−0.346

Al₃Sm, $\alpha(\beta)$ -Al₄Sm, Al₁₁Sm₃, and Al₅Sm, we also included several other low-energy structures with ~50 atoms/unit cell, which were identified in a comprehensive genetic-algorithm search through configurational space [6]. All these structures shown in table 1 were fully relaxed using density functional theory (DFT) with the VASP package. The generalized gradient approximation proposed by Perdew, Burke, and Ernzerhof [9] was used for the exchange-correlation functional. The electron–ion interaction was treated with the projector-augmented wave method [10]. A cutoff energy of 400 eV was used for the plane-wave basis. The total-energy converged to 10^{-5} eV per cell in each self-consistent loop, and structural relaxation was terminated when the force on each atom fell below $0.01 \text{ eV } \text{\AA}^{-1}$. Since Sm adopts a valence of 3 in most compounds, we chose a pseudopotential for Sm that includes only one 4*f* electron

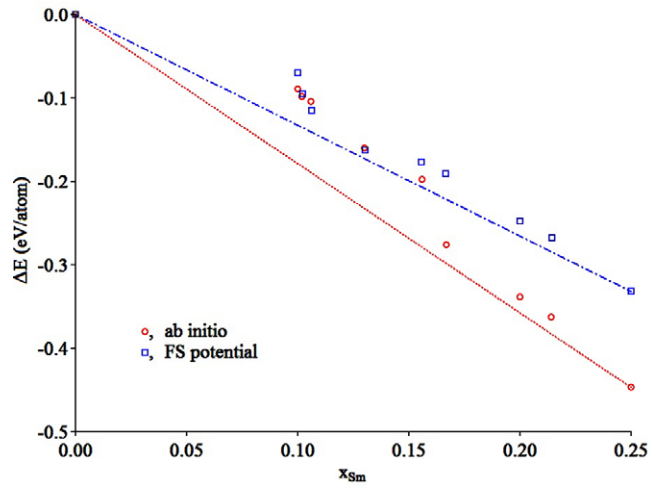


Figure 1. Formation energies of the most stable crystal phases in the Al–Sm alloy at $T = 0$ K. The reference states are pure Al and Sm.

in the valence configuration (i.e. the outer shell configuration is $4f^1 6s^2$). This pseudopotential successfully predicts that a rhombohedral structure for pure Sm is more stable than other lattice structures seen in early rare-earth elements. The formation energies of these structures calculated with respect to fcc Al and trigonal Sm are shown in figure 1.

To generate a model of the liquid $\text{Al}_{90}\text{Sm}_{10}$ alloy, we performed *ab initio* molecular dynamics simulations as implemented in the VASP package [11]. A large unit cell containing 500 atoms was used to ensure that the pair correlations of the system, especially those between the sparse species Sm, were captured with sufficient accuracy. Simulations were performed in the NVT ensemble, in which the number of atoms, volume, and temperature were held constant through the application of a Nose–Hoover thermostat. The Verlet algorithm was used to integrate Newton’s equations of motion, using a time step of 3 fs. We first equilibrated the model at 2000 K over 2,000 MD steps. Then, the sample was gradually cooled to 1273 K at a rate of $8.3 \times 10^{13} \text{ K s}^{-1}$.

3. Potential development procedure

When a semi-empirical potential is developed for an alloy, the traditional approach is to start by developing potentials for the pure elements (or to take these potentials from the literature) and then to fit the cross-functions (e.g. see [12–14]). When successful, this approach can lead to a potential suitable for a broad set of applications; however, it seems to be too involved for the purposes of the present study, which focuses on a very narrow concentration region. For instance, whether or not a potential is able to reproduce the properties of pure Sm is not important for the simulation of solidification/devitrification in $\text{Al}_{90}\text{Sm}_{10}$ alloy, because Sm never appears in these transformations. For this reason, we focused mostly on the different phases with approximately 10% Sm content in the potential development procedure. Nonetheless, we included some basic properties of pure Al (listed in table 2), as well as the formation energies of a few crystal phases with higher Sm content (listed in table 1). However, less weight was given to fitting these properties in the potential development procedure.

Table 2. The properties of pure Al used in the development of the FS potential^a.

Property	target value	FS potential
E_{coh} (fcc) (eV/atom)	− 3.362	− 3.905
C_{11} (GPa)	118	117
C_{12} (GPa)	62	63
C_{44} (GPa)	33	41
E_f^v (unrelaxed fcc) (eV/atom)	0.66	0.85
E_f^i (<100> fcc) (eV/atom)	2.43	2.73
$\Delta E_{\text{fcc} \rightarrow \text{bcc}}$ (eV/atom)	0.100	0.092
$\Delta E_{\text{fcc} \rightarrow \text{hcp}}$ (eV/atom)	0.028	0.019
T_m (K)	933	914
ΔH_m (T_m) (eV/atom)	0.108	0.102
$\Delta V_m/V_{\text{fcc}}$ (T_m) (%)	6.5	6.3

^a The references to target properties can be found in [21].

Formation energies of compounds strongly influence the driving forces for phase transformation, and so care was taken to reproduce these values for all relevant competing phases. The relative density of these phases is less important for our purposes, as long as residual stresses that develop during the transformation do not influence the transformation pathway, and so only the pure Al lattice parameter was included directly in this potential development procedure. We also included the density of liquid Al at the melting temperature T_m , and the density of liquid Al₉₀Sm₁₀ alloy at $T = 1273$ K, as obtained from *ab initio* molecular dynamics (AIMD).

Any semi-empirical potential that is to be used for modeling atomistic processes relevant to phase transformations that occur during solidification/vitrification should correctly reproduce the structure of the liquid/glass phase. The structure data can be obtained either from x-ray diffraction experiments or from *ab initio* molecular dynamics simulation. Since these data can be inconsistent with each other [15], and the developed potential incorporates much data obtained from AIMD calculations, in the present work we used only the AIMD liquid structure data. The procedure to fit an FS potential to target PPCFs followed in this work was proposed in [16]. It should be noted that while it is straightforward to determine AIMD PPCFs for a liquid alloy, accurate determination of PPCFs for a glassy system is much more difficult because the structural relaxation times required can sometimes exceed timescales accessible to even classical MD simulation [17]. Thus it is better to use AIMD PPCFs for a liquid alloy at a temperature which is low enough that specific features of the alloy structure are vivid but high enough that AIMD is able to reach the equilibrium structure at this temperature. In the present study we used AIMD PPCFs obtained at $T = 1273$ K as the target functions.

The potential development procedure used in the present study has been well documented in our previous works (for details, see [14] and references therein). The developed potential can be obtained in LAMMPS [18, 19] format from [20] and supplementary materials (stacks.iop.org/MSMSE/23/045013/mmedia). The potential functions are shown in figure 2. They look typical for FS potential functions. Effective pair potentials are frequently defined as

$$\varphi_{st}^{\text{eff}}(r) = \varphi_{st}(r) + \left(\left. \frac{\partial \Phi_s}{\partial \rho} \right|_{\rho_s} + \left. \frac{\partial \Phi_t}{\partial \rho} \right|_{\rho_t} \right) \psi_{st}(r), \quad (3)$$

where ρ_s is the value of ρ for component s in a particular phase. The effective pair potentials shown in figure 2 are calculated for the Al₃Sm phase. We note the rather smooth character of these functions.

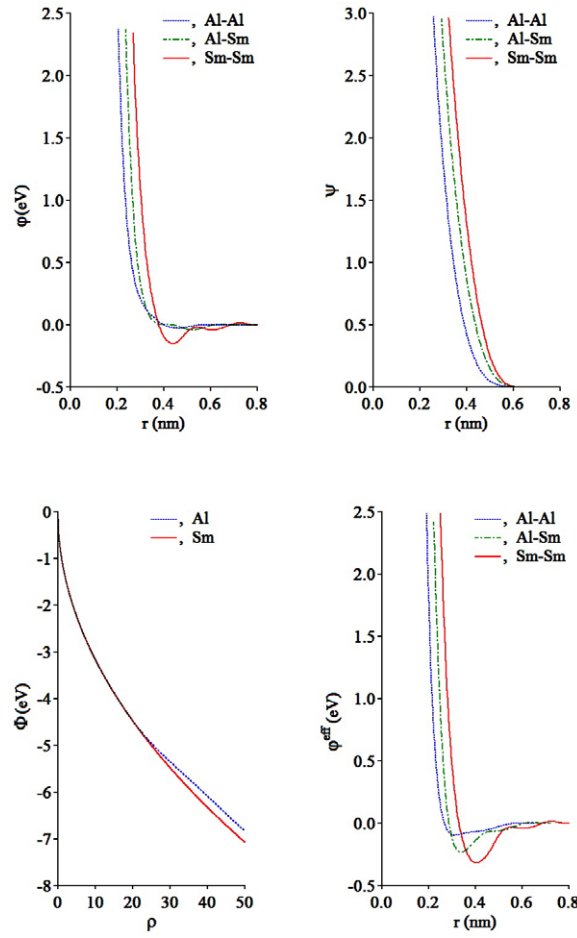


Figure 2. The developed potential functions. The effective potentials are calculated for the Al_3Sm phase.

Examination of table 2 shows that the basic properties of pure Al are reproduced reasonably well with this potential (although a specially developed potential can provide a much better agreement with the target Al properties [21]). The most pronounced disagreement between the target and reproduced Al values is for the cohesive energy. This should not be problematic unless the potential is used for the simulation of evaporation (see also the discussion in [22]). The developed potential ensures that all included crystal Al–Sm phases are metastable with respect to a mixture of pure Al and Al_3Sm in accordance with the experimental phase diagram and *ab initio* data (see figure 1). However, the potential considerably underestimates the absolute value of the formation energy of Sm-rich compounds.

Examination of table 1 shows that the potential provides reasonable values for the lattice parameters for most of the Al–Sm crystal phases even though they were not included in the potential development procedure. To find out which of these phase are at least mechanically stable at $T = 300\text{ K}$ we performed NpT (constant number of atoms, pressure and temperature) MD simulations where a barostat was used to ensure that all components of the stress tensor were zero. The simulation cells contained 1200–1800 atoms and the simulation time was 1 ns. Since any first-order phase transformation requires nucleation of a new phase, there is little

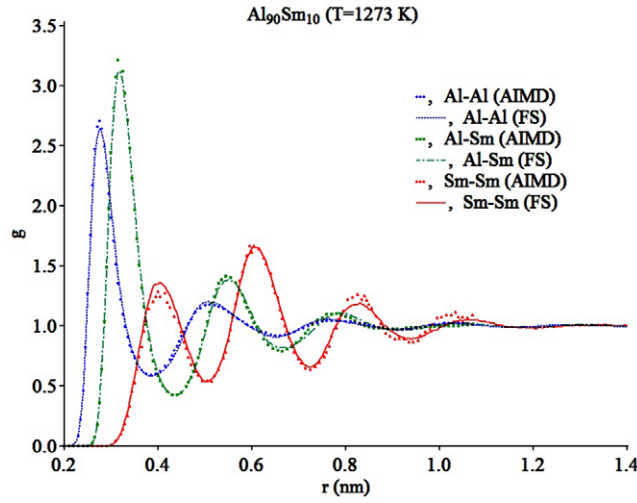


Figure 3. Partial pair correlation functions of liquid $\text{Al}_{90}\text{Sm}_{10}$ alloy at $T = 1273$ K.

chance of observing such a transformation during such short time simulations containing so few atoms. However, if a structure is mechanically unstable it will spontaneously transform to a mechanically stable structure. Thus, this test permits determining whether a given crystal phases is at least mechanically stable (metastable) at a particular temperature. These simulations showed that among all phases listed in table 1 only $\beta\text{-Al}_{40}\text{Sm}_8$ is mechanically unstable at $T = 300$ K.

Figure 3 shows that the PPCFs obtained with the developed potential are in very good agreement with the AIMD data. In particular this includes the very important fact that the height of the first peak of the Sm–Sm PPCF is smaller than that of the second peak (see [23] for more discussion). Thus, overall the developed potential satisfactorily reproduces all target properties included in the potential development procedure, especially taking into account that the main focus of the present work is the $\text{Al}_{90}\text{Sm}_{10}$ alloy.

It should be noted that the developed potential was not designed for simulation of alloys with the Sm content larger than 25% (no data for large Sm content were used in the potential development procedure). For example, the developed potential predicts that the most stable phase in Sm has the body-centered tetragonal lattice while both experiment and *ab initio* calculations show that the most stable phase in Sm has the rhombohedral lattice.

4. Simulation of liquid-glass transition

In order to determine the liquid-glass transition temperature T_g in the $\text{Al}_{90}\text{Sm}_{10}$ alloy, we created a liquid model containing 5000 atoms. The model was equilibrated for 40 ps at $T = 1100$ K using *NpT* MD simulation and then cooled down to $T = 300$ K using *NpT* MD simulation at a rate of 10^{10} K s^{-1} . The energy of the model as function of temperature is shown in figure 4. The shape of the curve shown in this plot is typical for systems that are quenched through a glass transition (see, e.g [14]). At low temperatures, atomic motion closely resembles simple harmonic vibration, such that the energy can be written as $E = E_0 + 3k_B T$ where E_0 is the energy at $T = 0$ K. Therefore, the value of $E - 3k_B T$ is largely temperature-independent, as can indeed be seen in figure 4. At higher temperatures, the anharmonicity of the atomic vibrations becomes increasingly important, and this leads to a corresponding increase

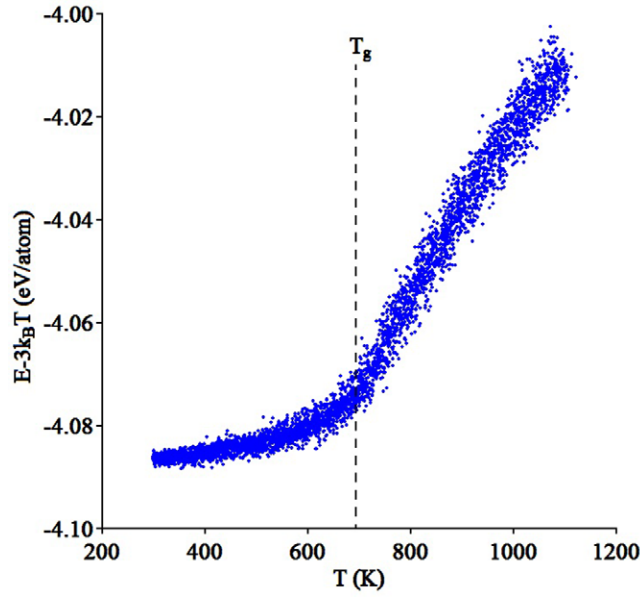


Figure 4. Total energy of the $\text{Al}_{90}\text{Sm}_{10}$ disordered alloy as function of temperature.

in the value $E - 3k_{\text{B}}T$, though the atomic motion is on the whole still oscillatory. In the liquid state, on the other hand, the quantity $E - 3k_{\text{B}}T$ depends strongly on temperature, because the harmonic approximation breaks down when atoms no longer vibrate around equilibrium positions. The glass transition temperature T_{g} separates these two regimes. There is no unique way to determine this temperature from MD simulation data. In the present work, we used the same method as in [14] and obtained $T_{\text{g}} = 693$ K.

The experimental value of T_{g} as determined from differential scanning calorimetry (DSC) for the Al–Sm alloy with a roughly 90–10 composition is 445 K [1]. This value is much lower than that obtained in MD simulation using the developed potential. The reason for this disagreement is not clear. One possibility is that the AIMD may overestimate the order in Al–Sm liquid alloys (*cf.* [15]) and the semi-empirical potential was fit to the AIMD PPCFs. It should also be noted that in the case of aluminum–rare earth alloys the DSC signal associated with the liquid–glass transition is very weak [24]. Thus, this question deserves further consideration.

5. Simulation of glass structure

To investigate whether the developed potential is able to predict properties beyond those which were explicitly included in the potential development procedure, we performed the following test. As was noted above it is very difficult to produce a well-relaxed glass model using AIMD. On the other hand it is not computationally expensive to determine the energy of a given atomic configuration from *ab initio* calculations (below we will refer to this quantity as the *ab initio* energy). In the case of glass, there are two obvious approaches to produce such a configuration [25]. In the first (purely *ab initio*) approach, a glass model is created by cooling a liquid model to $T = 0$ K using only AIMD. This method is limited to rather high cooling rates. In the second (hybrid) approach, a semi-empirical potential is employed to create a glass model at $T = 0$ K using a much lower cooling rate. Then the *ab initio* atomic forces are minimized and the *ab initio* energy can be calculated. If a semi-empirical potential provided

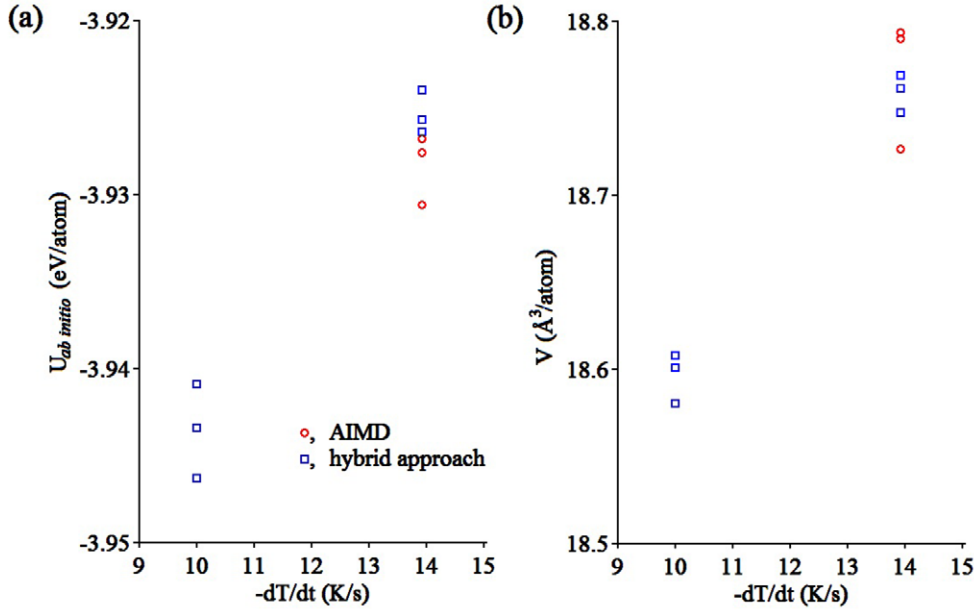


Figure 5. The (a) *ab initio* energies and (b) the atomic volume of the glass models at $T = 0$ K.

exactly the same atomic forces as the *ab initio* calculations, the *ab initio* energy of the hybrid model would be lower than that of the purely *ab initio* model due to the much lower cooling rates accessible through the hybrid approach. If the cooling rates were identical then it might be anticipated that of the two models the *ab initio* energy of the purely *ab initio* model would be lower because the atomic forces in the hybrid approach are less accurate. In general which model corresponds to lower *ab initio* energy depends on a competition between two factors: the cooling rate, and the quality of the semi-empirical potential. If the *ab initio* energy of the hybrid model is less than or equal to that of the purely *ab initio* model, then the potential can be considered as satisfactory.

In the present work, we used a liquid model composed of 500 atoms equilibrated at $T = 2000$ K for 6 ps. In the purely *ab initio* approach this model was cooled down to $T = 0$ K at a rate of $8.3 \cdot 10^{13} \text{ K s}^{-1}$. In the hybrid approach, the same initial model was cooled to $T = 0$ K using the developed FS potential at cooling rates of $8.3 \cdot 10^{13}$ and 10^{10} K s^{-1} ; then the *ab initio* atomic forces were minimized. In all cases, three runs corresponding to different initial atomic configurations at $T = 2000$ K were performed. The *ab initio* energies computed for these final models are shown in figure 5(a). For identical cooling rates, AIMD simulation produces configurations with lower *ab initio* energies than those obtained using the hybrid approach, as anticipated. However, when the hybrid approach is used to sample much lower cooling rates, the *ab initio* energies of the resulting configurations are considerably lower than values obtained using purely *ab initio* approach. The observed energy difference is about 15% of the pure Al latent heat. The atomic volumes in the glass models created using purely AIMD simulation and the hybrid approach are similar when the same cooling rate is used. However, for lower cooling rates the hybrid approach leads to higher atomic density than that achieved in the purely AIMD simulation (see figure 5(b)), which indicates more efficient atomic packing. Thus this test demonstrates the good quality of the developed potential.

6. Conclusions

In the present work we developed a semi-empirical potential for the $\text{Al}_{90}\text{Sm}_{10}$ alloy. The potential provides a satisfactory reproduction of basic pure Al properties as well as the formation energies of a set of Al–Sm crystal phases that contain about 10% Sm. Therefore the developed potential should provide reasonable estimations for the driving forces for phase transformations that occur in this composition range. The developed potential also closely reproduces the structure of the liquid $\text{Al}_{90}\text{Sm}_{10}$ alloy at $T = 1273$ K, in excellent agreement with AIMD simulation. Moreover, it leads to a glass structure with a lower *ab initio* energy than does the AIMD itself using cooling rates practical for AIMD simulations, which means that the developed potential should provide realistic liquid/glass structures at any temperature below $T = 1273$ K. Therefore, the developed potential should be suitable for the simulation of interfaces between crystal and liquid/glass phases. Based on these facts the developed potential can be used in MD simulations of solidification/vitrification in the $\text{Al}_{90}\text{Sm}_{10}$ alloy.

Acknowledgments

The authors are grateful to R T Ott, E Park, M F Besser and M J Kramer who performed experimental studies which motivated the present work and were heavily involved in the discussion of our simulation results. This work was supported by the U S Department of Energy, Office of Basic Energy Science, Division of Materials Sciences and Engineering, including the computer time allocations at the national energy research scientific computing center (NERSC) in Berkeley, CA. The research was performed at the Ames Laboratory. Ames Laboratory is operated for the U S Department of Energy by Iowa State University under Contract No. DE-AC02-07CH11358.

References

- [1] Wilde G, Sieber H and Perepezko J H 1999 *J. Non-Cryst. Solids* **250** 621
- [2] Massalski T B, Okamoto H and ASM International 1990 *Binary Alloy Phase Diagrams* 2nd edn (Materials Park, Ohio: ASM International)
- [3] Kalay Y E, Yeager C, Chumbley L S, Kramer M J and Anderson I E 2010 *J. Non-Cryst. Solids* **356** 1416
- [4] Kalay Y E, Chumbley L S, Kramer M J and Anderson I E 2010 *Intermetallics* **18** 1676
- [5] Mishin Y, Asta M and Li J 2010 *Acta Mater.* **58** 1117
- [6] Zhang F, McBrearty I, Ott R T, Park E, Mendelev M I, Kramer M J, Wang C Z and Ho K M 2014 *Scr. Mater.* **81** 32
- [7] Daw M S and Baskes M I 1984 *Phys. Rev. B* **29** 6443
- [8] Finnis M W and Sinclair J E 1984 *Phil. Mag.* **50** 45
- [9] Perdew J P, Burke K and Ernzerhof M 1996 *Phys. Rev. Lett.* **77** 3865
- [10] Vanderbilt D 1990 *Phys. Rev. B* **41** 7892
- [11] Kresse G and Furthmüller J 1996 *Comput. Mater. Sci.* **6** 15
- [12] Williams P L, Mishin Y and Hamilton J C 2006 *Modelling Simul. Mater. Sci. Eng.* **14** 817
- [13] Pasianot R C and Malerba L 2007 *J. Nucl. Mater.* **360** 118
- [14] Mendelev M I, Kramer M J, Ott R T, Sordet D J, Yagodin D and Popel P 2009 *Phil. Mag.* **89** 967
- [15] Kramer M J, Mendelev M I and Asta M 2014 *Phil. Mag.* **94** 1876
- [16] Mendelev M I and Srolovitz D J 2002 *Phys. Rev. B* **66** 014205
- [17] Zhang F, Mendelev M I, Zhang Y, Wang C Z, Kramer M J and Ho K M 2014 *Appl. Phys. Lett.* **104** 061905
- [18] Plimpton S 1995 *J. Comput. Phys.* **117** 1
- [19] <http://lammps.sandia.gov/>

- [20] Becker C A, Tavazza F, Trautt Z T and de Macedo R A B 2013 *Curr. Opin. Solid State Mater. Sci.* **17** 277 (www.ctcms.nist.gov/potentials)
- [21] Mendelev M I, Kramer M J, Becker C A and Asta M 2008 *Phil. Mag.* **88** 1723
- [22] Mendelev M I, Han S, Srolovitz D J, Ackland G J, Sun D Y and Asta M 2003 *Phil. Mag.* **83** 3977
- [23] Zhang F, Sun Y, Ye Z, Zhang Y, Wang C Z, Mendelev M I, Ott R T, Kramer M J and Ho K M in press
- [24] Kalay Y E, Kalay I, Hwang J, Voyles P M and Kramer M J 2012 *Acta Mater.* **60** 994
- [25] Mendelev M I, Kramer M J, Hao S G, Ho K M and Wang C Z 2012 *Phil. Mag.* **92** 4454